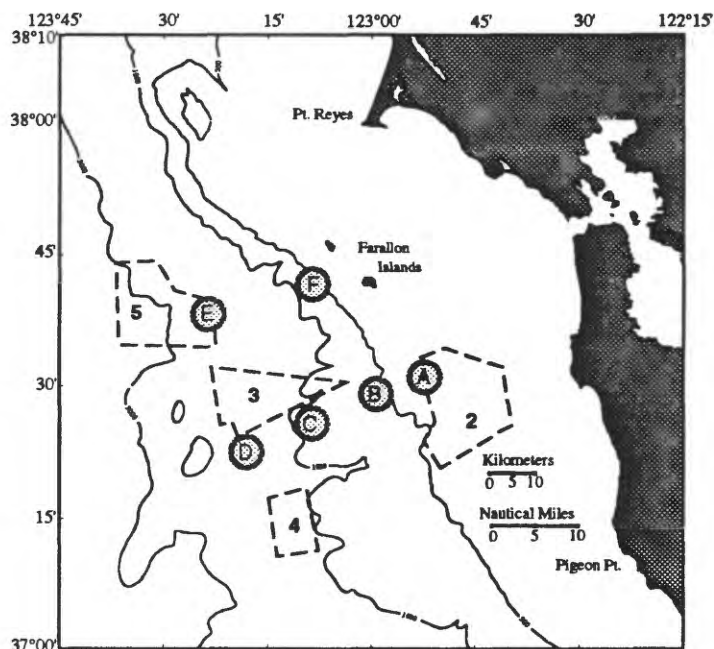


U.S. DEPARTMENT OF THE INTERIOR  
U.S. GEOLOGICAL SURVEY



Current patterns over the shelf and slope  
adjacent to the Gulf of the Farallones  
Executive Summary

by

Marlene Noble<sup>1</sup>, Steven R. Ramp<sup>2</sup> and Kaye Kinoshita<sup>1</sup>

Open-File Report 92-382

This report is preliminary and has not been reviewed for conformity with U.S. Geological Survey editorial standards or with the North American Stratigraphic Code. Any use of trade, product, or firm names is for descriptive purposes only and does not imply endorsement by the U.S. Government.

<sup>1</sup>U. S. Geological Survey, Menlo Park, CA, 94025

<sup>2</sup>Naval Postgraduate School, Monterey, CA, 93943

## TABLE OF CONTENTS

	Page
Introduction .....	1
Historical Perspective: Summary of Previous Work .....	4
The Moored Current-Meter Field Program .....	10
Description of the measured currents .....	10
Surface wind vectors .....	10
Currents over the outer shelf .....	10
Currents over the slope .....	12
Near-surface currents over the slope .....	12
Mid-depth currents over the slope .....	13
Deep currents over the slope .....	13
Near-bed currents over the slope .....	15
Discussion .....	15
Conclusions .....	17
References .....	18
Appendix .....	20
Subtidal current vector plots (Figures A - F) .....	21 - 26

## INTRODUCTION

In February 1991, a year-long study was begun of the circulation and related transport of suspended materials in the Gulf of the Farallones and over the adjacent continental slope. As part of this program, an array of current-meter moorings was deployed in the region. The information gathered in this study was designed to provide a basic description of the currents and an understanding of the underlying physical processes in the region so that models could be developed that will allow the Environmental Protection Agency (EPA) to choose appropriate sites for the deposition of materials dredged from San Francisco Bay. The observed currents will also be used with simple advection/dispersion models to allow EPA to predict the ultimate fate of materials deposited at those sites.

There are four primary sites of interest to the EPA, one on the shelf and three on the mid to outer slope (Figure 1). It was necessary to develop an extensive measurement program in the region so that the EPA could evaluate these sites because the historical data record is sparse. While currents have been monitored for several years on the shelf near candidate disposal site 2 (Strub et al., 1987; Sherwood et al., 1990), the historical data base for currents over the slope is almost nonexistent. It consists of a few short records collected mainly by the U. S. Navy in a variety of locations. Hence, the existing data records are too limited, both in duration and in spatial coverage, to provide the extensive knowledge necessary for the development of reliable transport models in the regions of interest.

The extensive, year-long field program begun in February 1991 gathered the data necessary to address the above issues. The program was developed and carried out by a consortium of agencies, companies and research institutions. Personnel from the EPA, U. S. Navy, U. S. Geological Survey (USGS), National Marine Fisheries, Naval Postgraduate School (NPS), Monterey Bay Aquarium Research Institute (MBARI), and Science Applications International Corporation (SAIC) cooperated in the design and execution of the project. The comprehensive program consisted of three elements. An array of moorings that collect measurements of current, temperature, salinity, and pressure was deployed for a year over the shelf and slope. Five quasi-synoptic surveys of the spatial structure of the currents above 300 m and the physical characteristics of the entire water column were conducted during February, May, August, and November 1991 and February 1992. Satellite images of the near-surface thermal structure were collected and processed. In addition, records of the wind velocity over the water and sea level height at the coast were

obtained from the National Data Buoy Office and the National Ocean Service.

In March, 1991, the moored array portion of the Farallones project was begun. SAIC and NPS deployed an extensive array of equipment at 6 sites, A through F, in the region of the Gulf of the Farallones (Figure 1, Table 1). The array was designed to monitor the current velocity, water temperature and several other physical characteristics of the water column for an entire year in order that seasonal changes in the measured parameters could be resolved. The selection of the exact locations for the measurement sites was based on several criteria. It was important to determine the spatial structure of the measured parameters and how that structure changed with time, depth and horizontal location. The array was designed to allow an evaluation of possible connections between the circulation and sediment transport patterns on the shelf and the slope. The locations were also chosen to provide information on characteristics of the circulation in candidate dredge disposal sites. The mooring sites are either adjacent to or within all areas of interest to the EPA.

The main line in the array, which contains sites A through D, monitors the changes in the physical oceanographic parameters with water depth. Changes in water depth typically cause the largest spatial gradients in the circulation and sediment transport pathways. Site A monitors currents and other properties of the water column in 92 m of water, a depth found on the outer shelf (Figures 1 and 2). Site B measures these same quantities in 400 m of water, over the upper slope. Sites C and D, located in 800 m and 1400 m of water, respectively, provide information on water movements over the mid and lower slope.

A primary purpose of the secondary line in the array, sites E and F, is to provide information on how the characteristics of the circulation patterns change with distance along the isobaths. Mooring F is in 400 m of water, the same depth but displaced from mooring B (Figures 1 and 2). Mooring E is paired with mooring D. Mooring E is also located on the inshore edge of candidate disposal study area 5, the most northerly of the possible disposal sites.

Each mooring in the array had between 3 and 6 instruments that measured current and temperature at specific locations in the water column (Figure 2). At selecte sites, some of the instruments also measured salinity (or conductivity) and pressure (Table 1). At each site, the instrument location was designed to resolve the expected vertical structure of the current and temperature fields. The instruments were closely spaced in the upper portions of the water column, where the vertical gradients were expected to be strongest (Figure 2, Table 1). The distance between instruments more than doubled in the lower

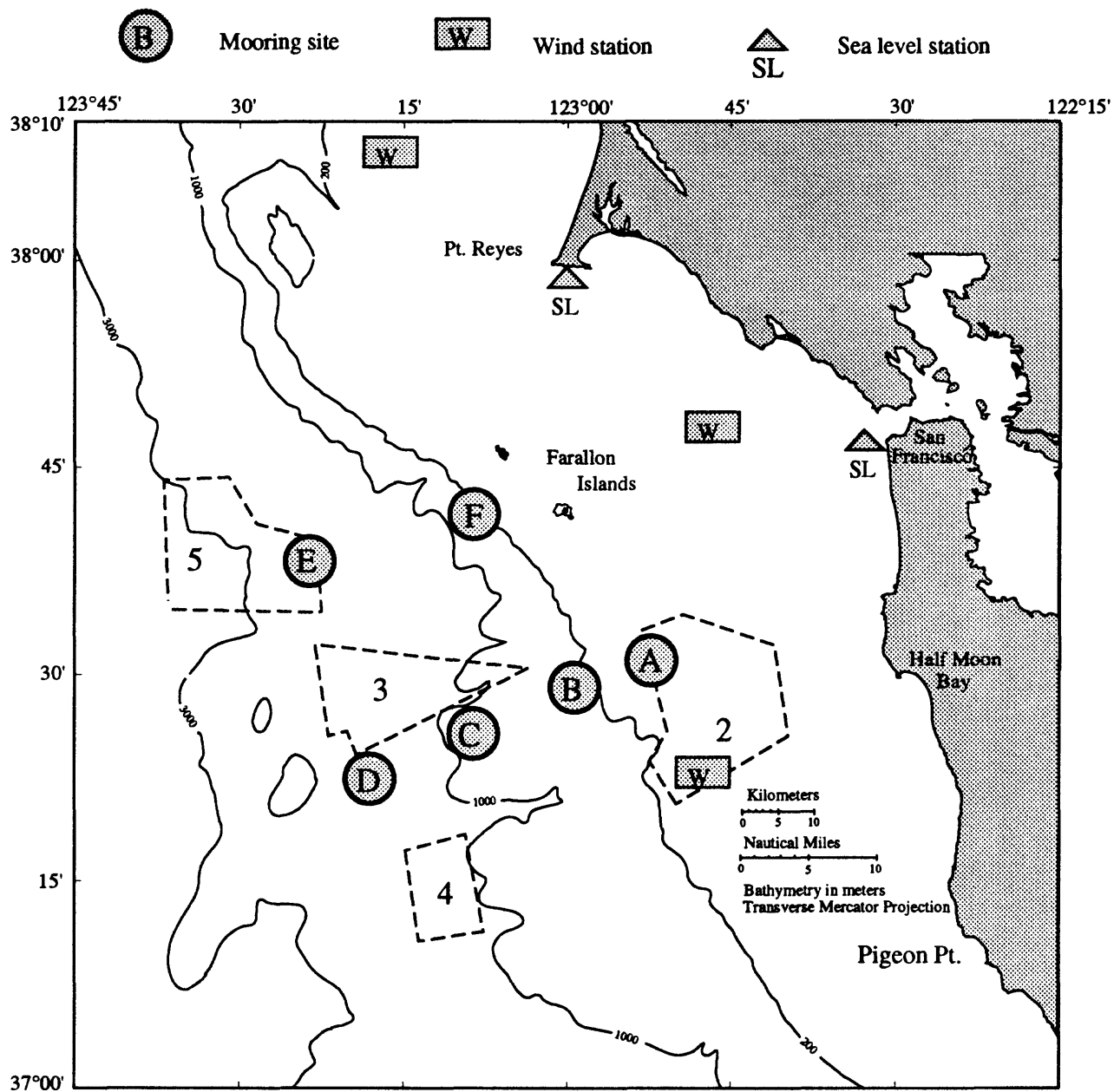


Figure 1. The locations of moorings A-F and the approximate location of EPA candidate disposal sites 2-5.

SITE	WATER DEPTH (m)	START TIME (M/D/Y)	STOP TIME (M/D/Y)	DATA FILLED IN		INSTRUMENT	POSITION		SENSOR DEPTH (m)	DATA TYPE	CURRENT DATA SAMPLE INTERVAL (MINUTES)	TEMP/SALINITY DATA SAMPLE INTERVAL (MINUTES)
				FROM APPROX. (M/D/Y GMT)	TO APPROX. (M/D/Y GMT)		LATITUDE	LONGITUDE				
A	92	03/08/91	01/05/92	---	---	S4	37 32.69 N	122 51.24 W	10	C, T, S	30	30
A	92	03/08/91	02/08/92	---	---	S4	37 32.69 N	122 51.24 W	50	C, T, S	30	30
A	92	03/08/91	08/13/91	---	---	S4	37 32.69 N	122 51.24 W	80	C, T, S	30	30
B	400	07/04/91	09/23/91	---	---	VMCM	37 28.63 N	122 59.76 W	10	C, T,	3.75	*1T=40, *2T=150
B	400	03/09/91	02/08/92	08/13/91 1800	08/14/91 2200	ACM2	37 28.71 N	123 00.30 W	150	C, T	*1=4, *2=15	*1T=40, *2T=15
B	400	03/09/91	02/08/92	08/13/91 0300	08/14/91 2100	RCM4	37 28.71 N	123 00.30 W	260	C, T, S	30	30
B	400	03/09/91	02/08/92	08/06/91 1600	08/14/91 2100	RCM4/5	37 28.71 N	123 00.30 W	390	C, T, S	30	30
C	800	03/09/91	02/09/92	---	---	VMCM	37 25.29 N	123 08.10 W	10	C, T	*1=4, *2=4, *3=30	*1=4, *2=4, *3=30
C	800	03/09/91	02/09/92	10/30/91 1600	10/31/91 0100	S4	37 25.29 N	123 08.10 W	75	C, T, S	30	30
C	800	03/09/91	08/13/91	---	---	ACM2	37 25.72 N	123 08.03 W	150	C	4	-
C	800	03/09/91	08/13/91	---	---	RCM4	37 25.72 N	123 08.03 W	250	C, T, S	30	30
C	800	03/09/91	09/11/91	---	---	RCM5	37 25.72 N	123 08.03 W	400	C, T, S	30	30
C	800	03/09/91	03/11/92	---	---	RCM5	37 25.72 N	123 08.03 W	790	C, T, S	30	30
D	1400	03/10/91	02/13/92	10/30/91 1600	10/31/91 2300	S4	37 21.19 N	123 16.20 W	75	C, T	30	30
D	1400	03/10/91	09/03/91	08/13/91 1400	08/14/91 1800	RCM4	37 21.83 N	123 16.05 W	250	C, T	30	30
D	1400	03/10/91	02/13/92	08/13/91 1500	08/14/91 2000	RCM5	37 21.83 N	123 16.05 W	400	C, T, S	30	30
D	1400	03/10/91	02/13/92	08/13/91 1300	08/14/91 1800	RCM5	37 21.83 N	123 16.05 W	800	C, T, S	30	30
D	1400	08/14/91	02/13/92	---	---	RCM5	37 21.83 N	123 16.00 W	1390	C, T, S	30	30
E	2040	03/11/91	04/16/91	---	---	VMCM	37 38.39 N	123 18.03 W	75	C, T	4	4
E	2000	03/11/91	08/15/91	---	---	RCM8	37 38.39 N	123 18.03 W	272	C, T, S, P	60	60
E	2000	03/11/91	02/12/92	---	---	RCM8	37 38.39 N	123 18.03 W	420	C, T	60	60
E	2000	03/11/91	02/12/92	---	---	RCM8	37 38.39 N	123 18.03 W	820	C, T	30	60
E	2000	03/11/91	02/12/92	---	---	RCM8	37 38.39 N	123 18.03 W	1400	C, T	30	60
E	2000	03/11/91	02/12/92	---	---	RCM8	37 38.39 N	123 18.03 W	1987	C, T	30	60
F	400	03/11/91	02/10/92	10/31/91 1600	10/31/91 1900	S4	37 41.97 N	123 08.63 W	75	C, T	30	30
F	430	03/12/91	02/13/92	---	---	S4	37 41.97 N	123 08.63 W	180/222	C, T, S, P	30	60
F	430	03/11/91	02/13/92	---	---	RCM8	37 41.97 N	123 08.63 W	280/322	C, T, S, P	30	60
F	430	03/11/91	02/13/92	---	---	RCM8	37 41.97 N	123 08.63 W	417/459	C, T, S, P	30	60

Table 1: Data availability for all moorings

C = Current data \* Deployment No.  
T = Sea Temperature  
S = Salinity  
P = Pressure

ACM2 = Neil Brown Acoustic Current Meter  
S4 = InterOcean S4  
VMCM = EG&G Vector Measuring Current Meter  
RCM4, RCM5, RCM8 = Aandera

SAIC = Science Applications International Corporation  
NPS = Naval Post Graduate School, Monterey, CA

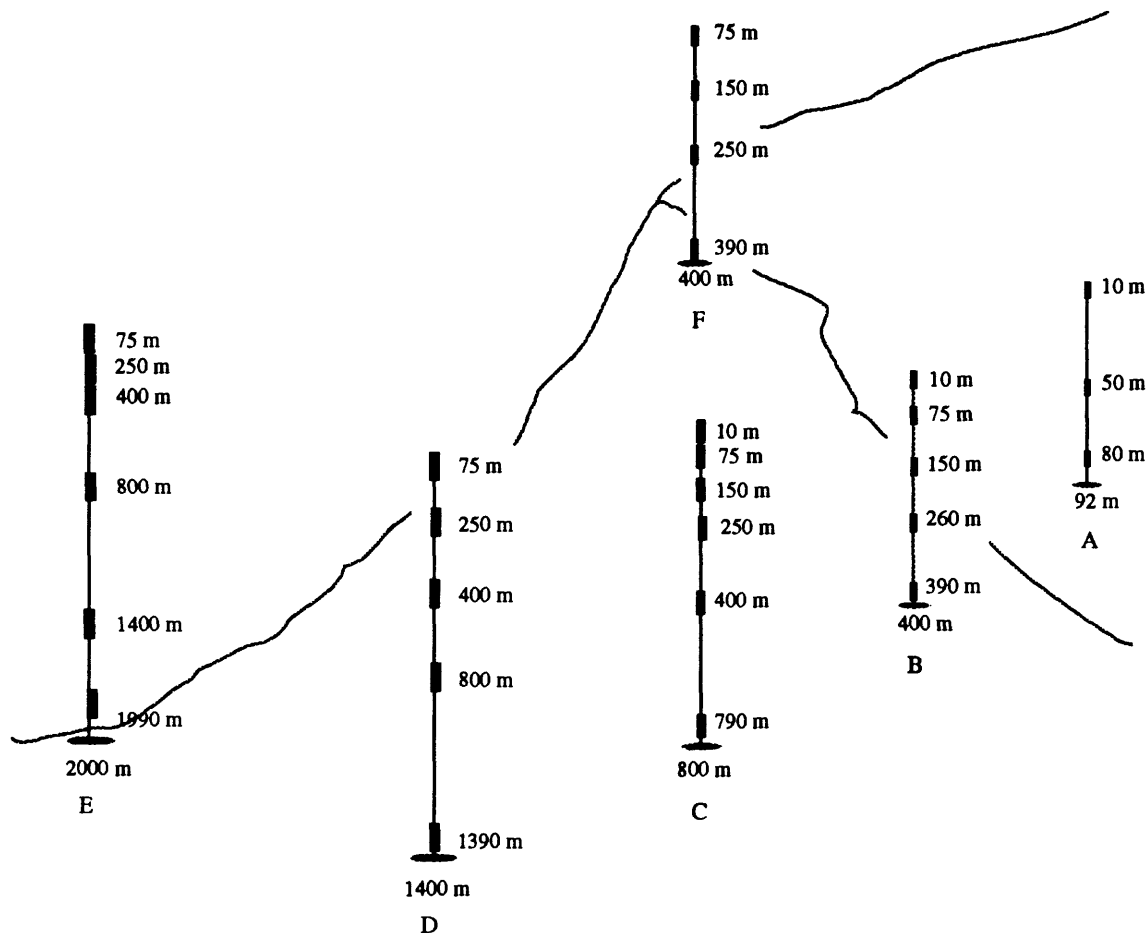


Figure 2. Location of instruments in the moored array

half of the moorings, where vertical gradients were expected to be smaller. Instruments on all the moorings were placed at similar water depths in order to resolve changes in the horizontal structure of the circulation patterns with depth (Figure 2, Table 1). Currents in the upper 75 m of the water column were monitored at all locations by 1 or 2 instruments. Other common instrument levels were 150 m, 250 m, 400 m and 800 m. In addition, all moorings had instruments within 12 m of the sea floor in order to monitor the strength of currents that could possibly resuspend deposited dredged materials. Unfortunately, not all of the instruments in the moored arrays worked and a more limited data set than planned was collected (Figure 3).

The next section of this report is a review of the present knowledge of circulation off the California coast. A subsequent section will describe the experiment and data handling. Discussions of the circulation patterns measured over the shelf and slope during this field program and the influences of the

currents on the possible resuspension and transport of materials in the region will follow.

### Historical Perspective: Summary of Previous Work

The study area lies within the California Current System, an eastern boundary current in the Northeast Pacific Ocean. This current forms the eastern limb of the North Pacific subtropical gyre, which is bounded on its southern, western, and northern sides by the North Equatorial Current, the Kuroshio, and the Kuroshio Extension/West Wind Drift, respectively. Based on a climatological view, shown well for instance, in the dynamic height maps of Wyrski (1965), the expected mean flow in the upper few hundred meters in the California Current System is a slow equatorward current towards the southeast (less than 10 cm/s), although this has proven difficult to measure using modern techniques.

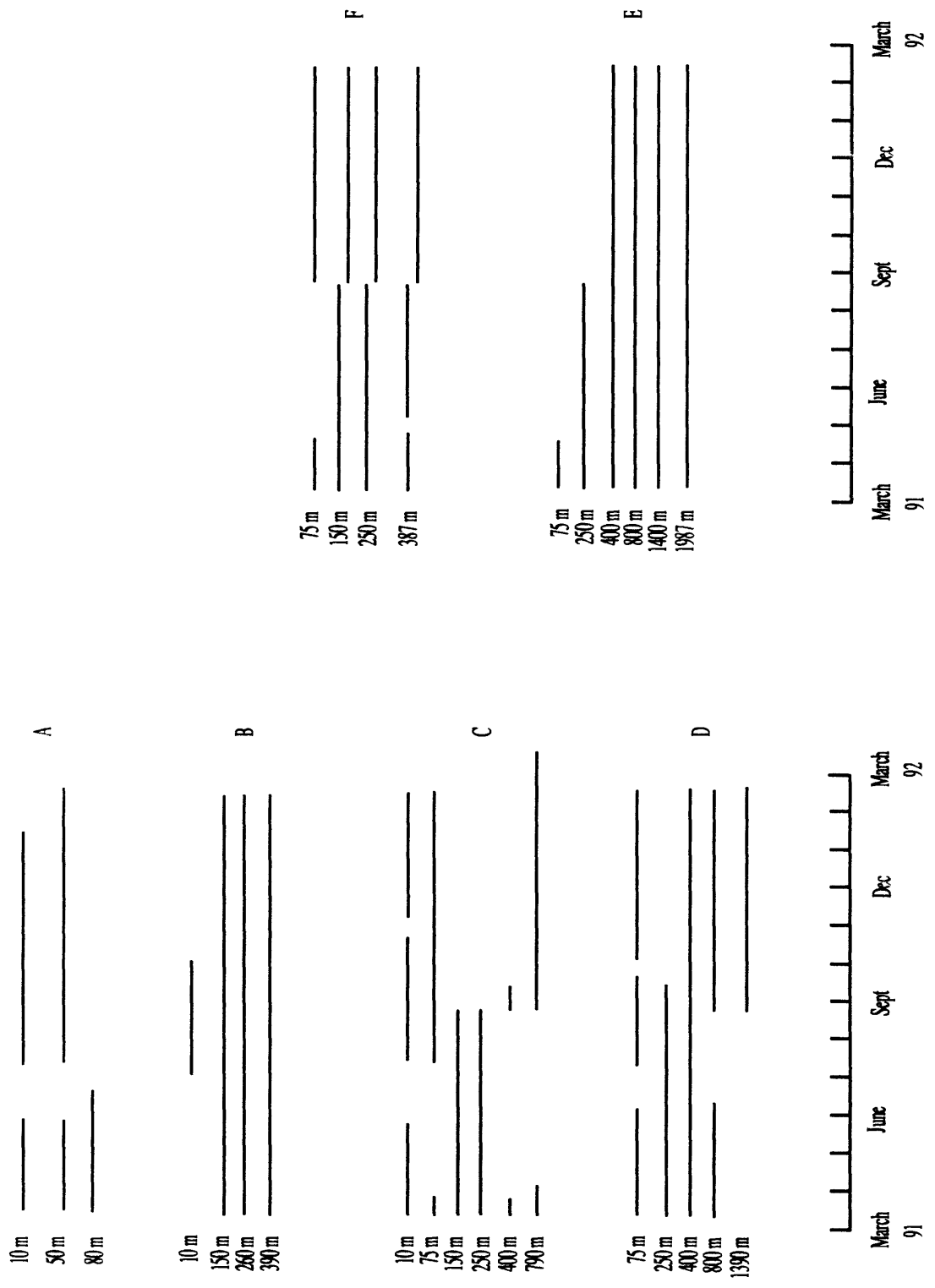


Figure 3. Timelines showing the dates when valid data from the current meters exists.

Perhaps the best evidence for a slow equatorward mean flow in the surface layers is provided by satellite-tracked drifter observations (Brink et al., 1991). These observations (Figure 4) are based on a true current-following satellite-tracked drifter with very little surface expression (i.e., it is not blown by the wind). The drifters show that a slow, equatorward mean flow is superimposed on a much more energetic mesoscale eddy field that disperses the drifters on the order of 200-400 km towards the east and west as they are slowly carried towards the south.

The eddy field embedded within the California Current System has been observed in several studies, such as the Coastal Transition Zone (CTZ) program (Brink and Cowles, 1991) and the Ocean Prediction Through Observations, Modeling, and Analysis (OPTOMA) program (Mooers and Robinson, 1984; Rienecker et al., 1987; Rienecker and Mooers, 1989). The eddy field is still poorly understood. We know that a vigorous eddy field exists, and sometimes interacts with the inshore waters. Eddies of a 30-50 km size range are sometimes observed over the continental slope, while the larger eddies (100-200 km diameter) seem confined to the offshore region. The eddy interaction is not well understood, but is presently being studied in much greater detail by the Office of Naval Research

(ONR) Mesoscale Interactions in Weakly Nonlinear Systems Accelerated Research Initiative (ARI).

Nested within the equatorward flowing California Current are two well known poleward flows (Hickey, 1979; Chelton, 1984; Neshyba et al., 1989), the Coastal Countercurrent and the California Undercurrent. Present knowledge of these currents was well summarized in recent review articles by Huyer et al. (1989) and Hickey (1989). The inshore coastal countercurrent has been observed both north and south of the our study area in the Gulf of the Farallones area, but not in the area because data has not been collected in this region. The best observations to the north were made during the Coastal Ocean Dynamics Experiment (Lentz, 1991) during 1981-82 along a relatively straight stretch of coast between Point Arena and Point Reyes, California. During the upwelling season (spring-summer), the countercurrent appeared whenever the equatorward upwelling favorable winds relaxed and disappeared (Send et al., 1987; Winant et al., 1987). The summer countercurrent was typically only 10-20 km wide, with velocities less than 30 cm/s (Kosro, 1987). The countercurrent is typically broader and stronger in the winter months (October - early March), when it sometimes covers the entire

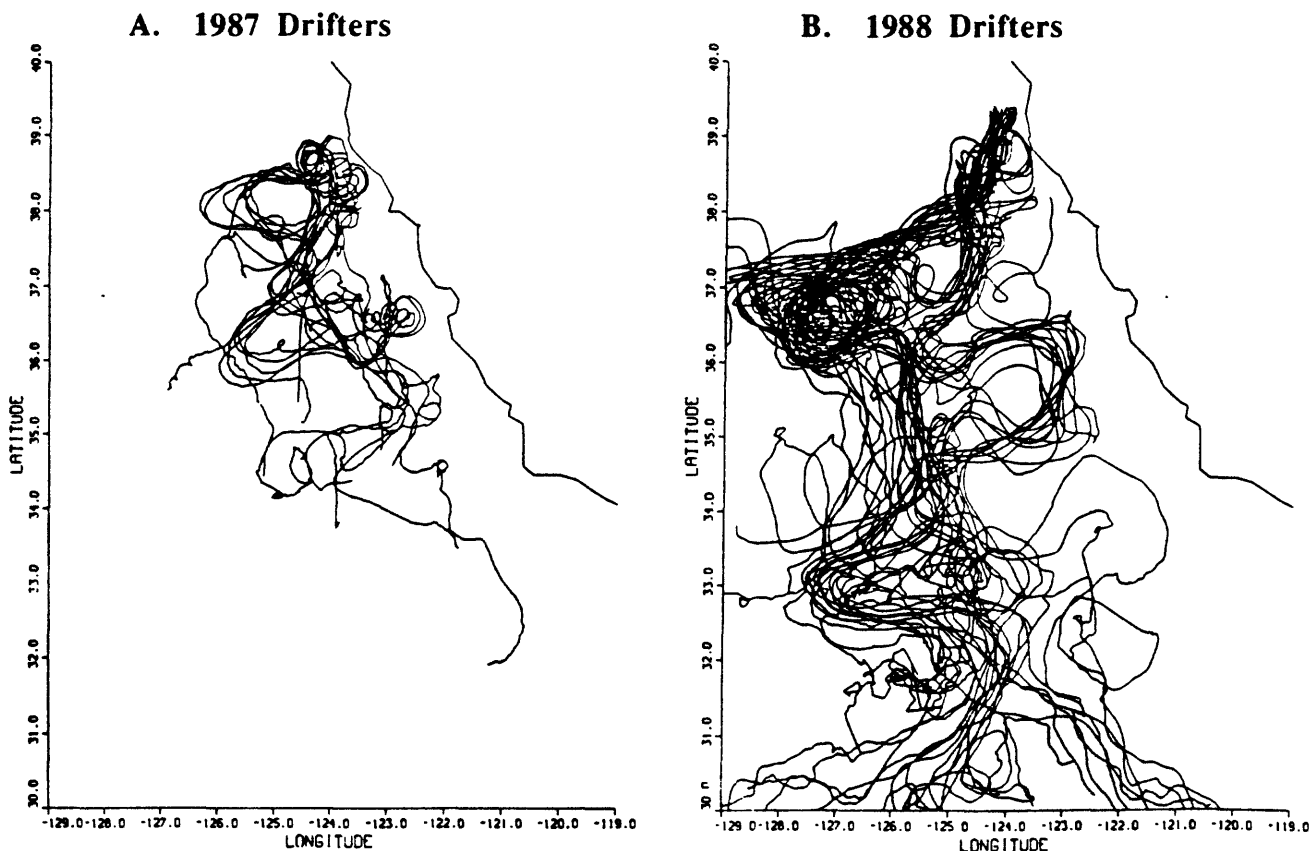


Figure 4. Complete (A) 1987 and (B) 1988 drifter tracks (Brink, et al., 1984).

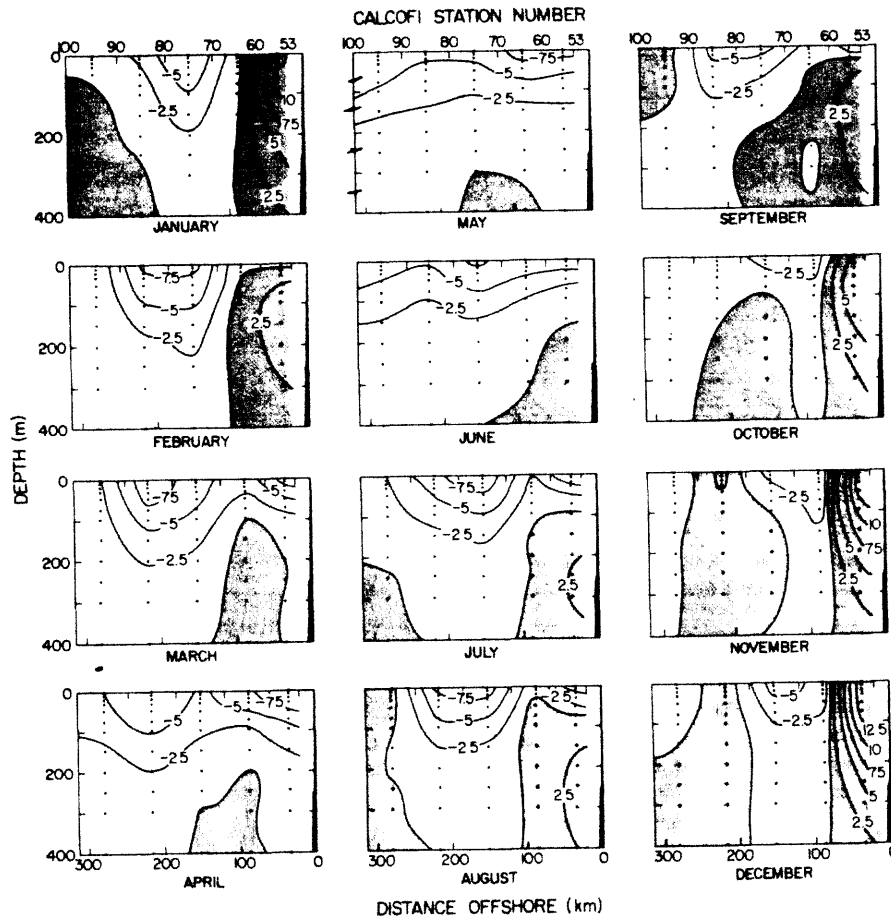


Figure 5. Vertical sections of seasonal alongshore geostrophic velocity relative to 500 dbar along CalCOFI line 70 off Point Sur. Shaded regions correspond to poleward flow (Chelton, et al., 1984) .

continental shelf and is known as the Davidson Current. Even in winter, the current remains strongest nearshore (Huyer et al., 1978).

The forcing mechanism for these nearshore poleward currents is not well understood. Two ideas often suggested are a poleward pressure gradient and positive curl of the equatorward wind stress, but the mechanism by which such an alongshore pressure gradient might arise is itself unclear. It is possible that alongshore variability of the alongshore wind stress causes a variable Ekman transport, which in turn sets down the coast more at some places than others. Another idea is that the north Pacific gyre imposes this alongshore pressure gradient at its eastern boundary.

The California Undercurrent is a strong poleward flow found over the slope. It has been observed everywhere along the coast where observations have been made including southern California (Lynn and Simpson, 1989), off Point Conception and Point Sur (Chelton, 1984; Chelton et

al., 1988; Tisch et al., 1991), Northern California (Freitag and Halpern, 1981), Oregon (Huyer et al., 1984; Huyer and Smith, 1985), Washington (Hickey, 1979), and Vancouver Island, British Columbia (Freeland et al., 1984). The position, strength, and core velocity of the undercurrent vary from place to place and at different times of the year, but we typically expect a maximum poleward velocity of around 30 cm/s between 150 to 300 m depth over the continental slope in water 500-1000 m deep. The CALCOFI data set, averaged over 23 years (Chelton, 1984) gives some idea of the spatial and temporal extent of the California Undercurrent off Point Sur (Figure 5). These observations lead us to expect a well-developed undercurrent will be found over the Farallones slope. Undercurrent dynamics are poorly understood, but poleward pressure gradient forces due to the variable surface wind stress are once again often cited (McCreary, 1987). This is an area deserving further research.

All the currents described above are mean flows in that they are fairly steady over periods of many months. However, the characteristics of the mean flows are subject to considerable interannual variability. The El Niño/Southern Oscillation (ENSO) events can alter the mean current field on a year-to-year basis, and evidence from the tropical Pacific indicates that 1991-1992 was an ENSO year. ENSO events can cause both anomalous atmospheric conditions and anomalous oceanic conditions in the northeast Pacific. Weakened equatorward winds or poleward winds may cause reduced upwelling and onshore transport, which leads to warmer than usual conditions. The ENSO events can also excite very low frequency wave motions at low latitudes which then propagate poleward into the northern hemisphere along the shelf and slope. While these motions have been generated in many numerical models (Parré-Sierra and O'Brien, 1990), very few data sets exist which are long enough to verify their presence. One example is Huyer and Smith's (1985) data, which showed that the northward flow over the shelf was twice as strong during the El Niño winter of 1982-1983 than during the preceding and subsequent "normal" years.

Coastal upwelling, which causes shelf water to exchange with slope water, is a basic feature of the circulation along the entire central coast. The mechanism of coastal upwelling is that the equatorward wind stress transports surface water away from the coast due to the earth's rotation (Huyer, 1983; Brink, 1983). This water is then replaced by cooler, saltier water that moves upward from below. A front forms between the cold, salty, denser freshly upwelled water and the warmer, fresher, less dense water further offshore. North of Cape Blanco, the upwelling front is fairly straight along the coast, but to the south, large meanders develop and form "cold filaments" of freshly upwelled water that extend more than 200 km offshore. The filaments are most commonly observed near coastal promontories such as Cape Mendocino, Point Arena, Point Reyes, and Point Sur (Figure 6). The Point Arena filament was observed in six different surveys during July and August 1988 (Huyer et al, 1991). The offshore velocities along the northern side of the filament approached 100 cm/s (2 knots) which is far greater than the large scale mean flow towards the south. The across-shore volume transport in filaments has been variously estimated at between  $3 - 4 \times 10^6 \text{ m}^3/\text{s}$  (Ramp et al., 1991). These large across-shore transports, both on- and offshore, are of particular importance to the candidate disposal sites. The Point Reyes filament is less studied and less well understood than its counterpart off Point Arena to the north. It is nevertheless reasonable to expect large across-shore transports to be associated with the Point Reyes feature as well, which can potentially impact

the candidate disposal sites. Because the filaments are associated with upwelling, they are not commonly seen in winter.

At the high end of the frequency spectrum, tidal currents over the shelf and slope are not insignificant and cannot be ignored. The strongest tidal current component is either the principal lunar or the luni-solar diurnal tide, which have periods of 12.42 hours and 23.93 hours respectively. The diurnal tides are strongest on the shelf in the Gulf of the Farallones (Noble and Gelfenbaum, 1990). Diurnal tidal amplitudes range between 6 and 9 cm/s. The lunar tidal currents are strongest on the slope adjacent to the Gulf of the Farallones, with amplitudes ranging between 2.3 cm/s and 4.4 cm/s at site E (Noble, 1990). The semidiurnal and diurnal tides together account for 35 to 60% of the total variability in the current records on the shelf and 15 to 33% of variability on the slope. These tidal currents assist in the resuspension of material deposited on the sea bed and act to disperse material suspended in the water column. Suspended material can be spread over 1 km during a 6 hour time period.

The historical database suggests that the circulation over the continental shelf and slope near the Farallon Islands can be summarized as follows. In the mean, the surface circulation from the shelf break seaward is likely equatorward during the upwelling season, with an amplitude less than 10 cm/s. The surface currents will be variable in the other seasons, with amplitudes and directions changing in part because the surface wind stresses are variable. Over the continental slope, at depths between 100 and 1000 m, the flow is likely to be poleward due to the presence of the California Undercurrent. It is probable that these currents flow poleward the year around, but their amplitude will be stronger at some times than others in a way that is not yet fully understood. Strong, persistent bursts will occur in the current measurements that have times scales of several months. The basic state flow thus described will be perturbed occasionally by the Point Reyes coastal upwelling jet, which sometimes swings southward and crosses the northern corner of the study area. The basic state will also be perturbed by occasional mesoscale eddies that move into the area. The mean currents will carry suspended materials mainly along the isobaths. The jets, eddies and tidal currents will disperse the suspended materials across isobaths.

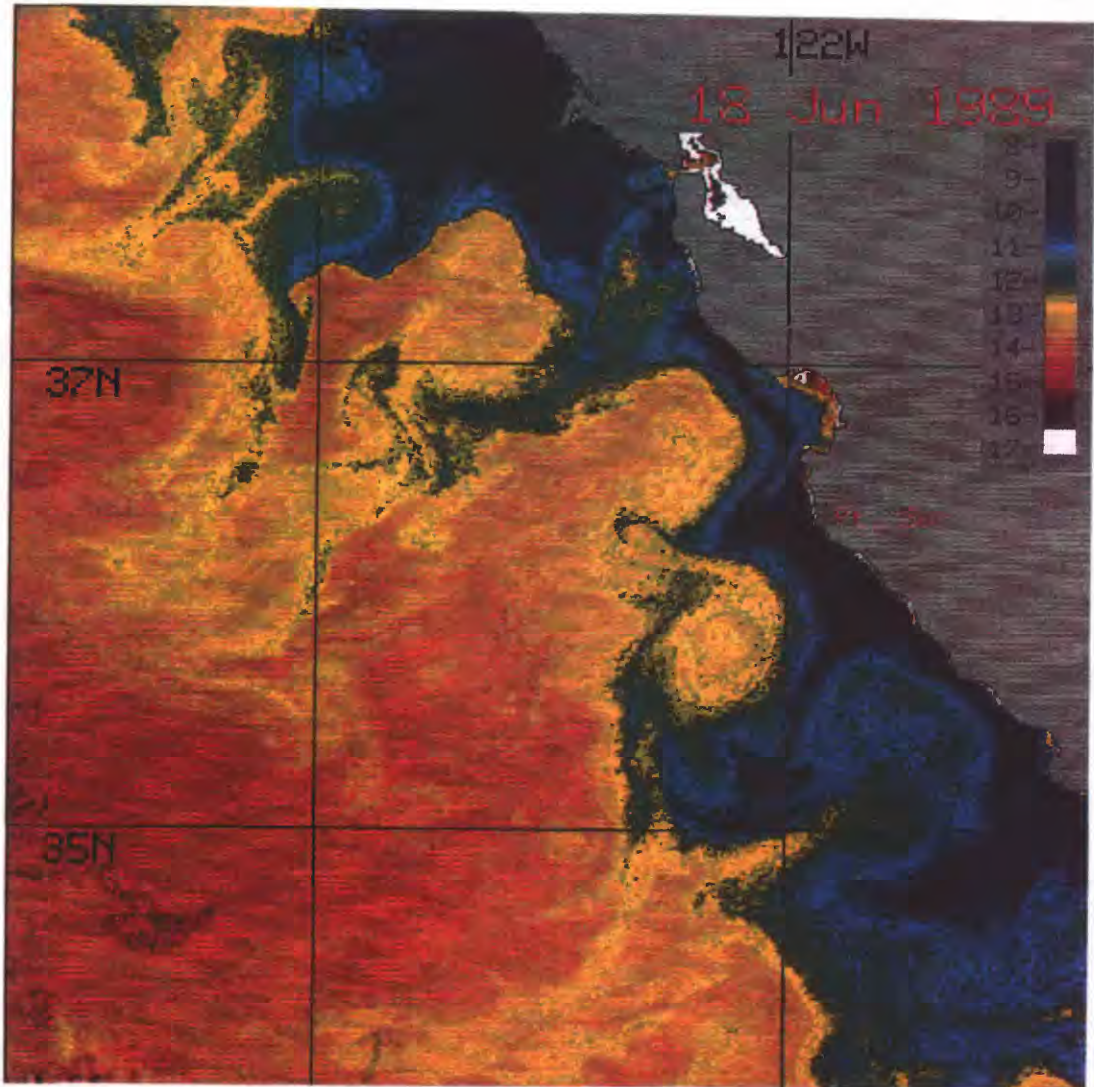


Figure 6. A filament off Point Sur, California.

On the shelf itself and inshore of the Farallon Islands, the expected flow will be closely coupled with the local surface wind stress, equatorward when the wind is equatorward, and poleward when the wind is slack or poleward. The flow here may also be affected by buoyancy driven flows due to the outflow from the San Francisco Bay. This aspect of the flow has not been studied previously and the magnitude of the effect is unknown. The tidal currents over the shelf are strongly diurnal and relatively important. Because currents due to waves generated during winter storms can reach depths of 100 m or more, fine grain material will not remain undisturbed over most areas of the shelf.

### **The Moored Current-Meter Field Program**

Six current-meter moorings were deployed on the shelf and slope in water depths that ranged from 90 to 2000 m (Figure 1). The moored array was designed to monitor the full range of circulation patterns describe in the background section. The main line, comprised of mooring A-D, measured currents from the shelf to the outer slope. The secondary line, comprised of moorings F and E, measured the changes in the circulation patterns with distance along the slope. Each mooring contained three to six instruments that were spread over the entire water column. To ensure a quality data product, specialized current meters, either EG&G vector-measuring current meters (VACMs), Interocean S4's or Neil Brown acoustic current meters (ACM2's), were deployed in the upper 150 m of the water column (Table 1). These current meters are designed to monitor current fluctuations even when currents from large surface waves are present. The current meters below 150 m were Aanderra RCM4, RCM5 or RCM8s, instruments that provide quality data at the deeper sites where currents from surface waves do not exist. The sampling intervals were chosen to be appropriate for the instrument depth and type (Table 1). The moored instruments were recovered and redeployed on 3 or 6 month intervals in order that an entire year of data could be collected at each site.

Some common conventions have been used to standardize the data sets collected in the program. Greenwich mean time (GMT) is used as the common time base for the data. All vector quantities, such as current and wind stress, have been rotated into a coordinate system that is aligned with the mean alongslope isobaths. Positive alongslope is toward  $328^{\circ}$ ; positive cross-slope is toward  $58^{\circ}$ . Two data records have been created for each instrument, an hour-averaged record and a subtidal record. The hour-averaged record is primarily used to analyze the tidal

constituents at each site. The subtidal record has the tides removed; the data is filtered so only fluctuations with periods longer than 33 hours remain. The subtidal records show the dominant circulation patterns over weekly and seasonal time scales.

There are temporal gaps in many of the data records, either because an instrument failed while it was deployed or because the instruments were out of the water during a replacement operation (Figure 3). Gaps of less than 2 days have been filled in with data either inferred from the measurements surrounding the gap or with measurements from near-by instruments.

### **Description of the measured currents**

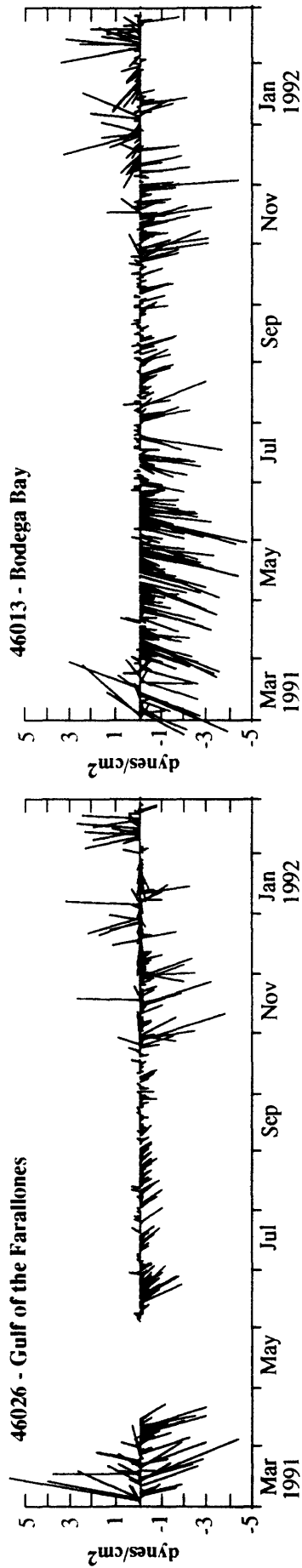
#### *Surface wind vectors*

The surface wind vectors for calendar year 1991 for the 4 offshore buoys near the study site (Figure 7) show how the near surface forcing changed during the year. The similarity of the four plots shows the large scale of the weather systems which passed through the area. The Bodega Bay data are likely representative (though slightly stronger) than the Gulf of the Farallones data when gaps in the data are present. The stronger winds at Bodega Bay and the Monterey Bay are likely because these two buoys are slightly farther offshore and less sheltered by land than the other two.

From January through early April, the winds were variable in both speed and direction. During the summer months, the usual upwelling favorable northwest winds of 10 to 15 m/s predominate. Winds during the fall were still mainly equatorward, but weaker than during the summer. Some wind reversals occurred, but were usually weak and lasted only a day. After the beginning of November, winter conditions similar to the beginning of the year returned, with strong, frequent reversals.

#### *Currents over the outer shelf*

Currents over the outer shelf were measured at site A, a site in 92 m of water that lies within one of the candidate disposal areas of interest to EPA (Figure 1). This site is close to historic measurement sites that have been occupied collectively for more than 2 years (Strub et al., 1987; Sherwood et al., 1990), so the measurements collected during this one year field program can be compared to current patterns observed during other years. Measurements of the near-surface and mid-depth currents were obtained for nearly the entire year of the program (Figure 3). Because of instrument failure, near-bottom currents were monitored for only the first 5 months of the deployment period.



11

\* Data was filled in from approximately 04/08/91 1000 to 07/30/91 0600 by running correlations between all the buoys for the 15 month time period that wind stress data existed. All correlations were greater than 0.88 for the alongslope winds. The best correlations were between 46012 and 46042. The energy levels in these two wind stress records were similar, also.

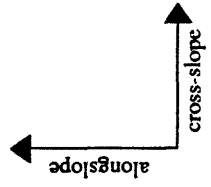
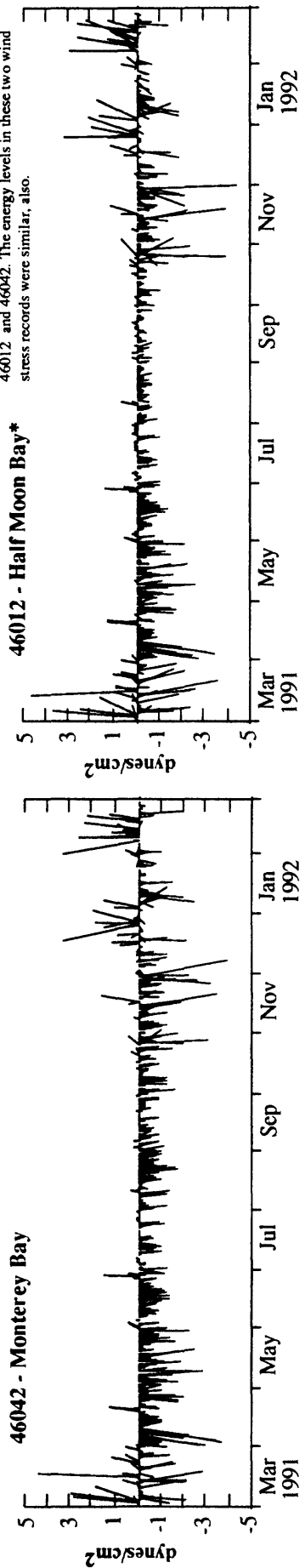


Figure 7. Lowpassed NODC wind stress vectors.

Vertical comparisons of the subtidal currents at site A are obscured by gaps in the data, but the available data suggest a vertically coherent flow during the first half of the year. The fluctuations in the alongshore component were visually quite similar and nearly uniform in magnitude with depth, weakening only slightly towards the bottom (Figure A). The correlations among the alongshelf currents at the three depths were 0.77 or larger over the year of record.

There was a tendency for the along isobath flow at mid-depth to veer toward the coast; the average mid-depth cross-slope flow was toward the coast with a mean speed of 2.4 cm/s. This steady cross-slope flow was not observed near the surface or near the bed. The cross-shore components were weak and were not coherent with depth.

The currents can only be compared at 10 and 50 m during the last half of the year, due to missing data at the bottom. From September to December, the currents were less vertically coherent. The 10-m currents were variable and tended to follow the wind stress (Figure A), while the 50 m flow was persistently poleward, often against the wind stress. As discussed earlier, this flow may be driven by poleward alongshore pressure gradient forces.

Comparisons between the outer shelf and upper slope currents (sites A and B) are difficult to make due to a lack of data at site B at 10 m depth (Figure B). The next site B depth, 150 m, is clearly in a different dynamical regime (see below) and is completely different than the shelf currents. Less than 15% of the variability in the alongslope flow at site B is related to that at site A. At 10 m, the short piece of data during July and August at site B is visually similar to site A, although this may not be true at other times. The record at site B is too short to allow statistical comparisons.

The tidal currents were the other strong component of the currents over the shelf. The principal diurnal tides and the principal semidiurnal tides can each have speeds of 8 to 9 cm/s (Kinoshita, et al., 1992). Hence, the tidal and subtidal currents can combine to generate strong currents. The maximum speeds over the shelf ranged between 40 and 60 cm/s. The maximum speed near the bed is 47 cm/s. These currents can be strong enough to move fine sand.

#### *Currents over the slope*

The extensive data set collected on the currents over the slope adjacent to the Gulf of the Farallones during 1991 and 1992 suggests that the currents in this region can be grouped into classes that are separated by depth ranges. Near-surface currents are those above 75 m depth. The mid-depth currents lie between 75 m and 800 m, provided that the deepest current associated with this category is at

least 50 m above the sea bed. The deep currents are found below 800 m and at least 50 m above the bed. The near-bottom currents are found 10 to 15 m above the sea bed. The currents within each category share similar characteristics and the coupling among currents within each category is much stronger than the coupling between currents in separate categories. Hence, the different categories will be discussed separately.

There is one strong caveat to the discussions presented below about the characteristics of currents within a category and the inferences about the relations between categories. A significant difference exists in the amount of information available in each category. The near-surface measurements were mainly collected at site C (Figure 3). Only a short record of near-surface currents is available at site B. The deep currents were only measured at site E (Figure 3). In contrast, records of mid-depth currents existed for large portions of the year at all sites on the slope. Often, a particular slope site would have several records of mid-depth currents between 75 and 800 m. At least 6 months of near-bottom currents were obtained at each site on the slope.

#### *Near-surface currents over the slope*

The near surface currents over the slope can only be well studied at site C. The spring currents here were characterized by a strong equatorward event during April (Figure C). This event reached at least 250 m at site C and cannot therefore be attributed to wind. This event is likely due to a mesoscale phenomenon such as the inshore edge of an anticyclonic (clockwise) eddy or a southward flowing upwelling filament. Further analysis of the hydrographic and satellite data will be necessary to confirm this hypothesis. Similar equatorward events were also observed at moorings D and E during this time, although it would be premature to attribute all three to the same physical cause. The depth of this event exceeded 800 m at the other two moorings. The strength and duration of the event at 250 m depth was about the same at moorings C and D.

Following a data gap, the flow at site C at 10 m depth was poleward at greater than 30 cm/s for the rest of the record, except for two flow relaxations that occurred during September 1991 and January 1992 (Figure C). A portion of this flow likely represents a surfacing of the California Undercurrent which is common during the fall and winter months. Once again, more analysis will be required to determine the cause of the relaxations.

The near-surface diurnal and semidiurnal tidal currents could have amplitudes up to 5 or 6 cm/s (Kinoshita, et al., 1992). Hence, the tidal currents generally did not have sufficient strength to reverse the dominant flow direction of the near surface

currents. The tidal currents can act to disperse materials suspended in the near-surface water, but they would not cause large changes in the fate of those materials.

#### *Mid-depth currents over the slope*

The subtidal, mid-depth currents over the slope form a wedge-shaped region of strongly correlated flow, both horizontally and vertically (Figure 8). Instruments included in this "wedge" include 150 and 260 m at site B; 75, 150, and 250 m at site C; 75, 250, 400, and 800 at site D; and 272, 420, and 820 m at site E. The majority of currents in this region flow along the isobaths. The inshore boundary of the wedge in the northern portion of the study region is offshore of that to the south. The offshore boundary of this flow field extends past the array and was not well delineated. Over 85% of the subtidal variability in alongslope currents in 250 m of water at site C is related to that at 150 m. During the first half of the year, when poleward flow was strongly evident, over 70% of the variability in alongslope currents between 75 and 400 m at site D was correlated. At site E, over 80% of the variability was correlated between 250 and 400 m.

This region is where the California Undercurrent has traditionally been found. Indeed, the most prominent feature here is a burst of strong (>30 cm/s) poleward flow lasting from mid-April to 1 September (Figures B-E). Interestingly, this event begins and ends about 5 days earlier in the north (Site E) than the south (Line B-D). The later start may be due to stronger influence of the preceding equatorward event in the south. Another possibility is that this represents a meandering current that moves onshore earlier in the north than the south. Similar bursts of poleward flow have been observed over the slope in longer, 3 year records off Point Sur, California (Ramp et al., 1991). Such bursts there were not phase-locked to the seasons. Hence, it is not clear if the poleward bursts observed in the data records collected off the Farallones are part of a seasonal cycle or if they appear randomly at different times in other years.

Both the persistent poleward flow and the strong vertical correlations in the subtidal alongslope currents weakened as the year progressed. At all sites, the mid-depth flow was reduced in amplitude and more erratic in direction from mid-August through mid-November (Figure F). The vertical correlations at sites B and D were reduced 20%. There was no mid-depth data collected at site C in the later portion of the year, but we expect that those currents would also weaken and become more erratic. Subsequently, there was a partial return to the strong poleward flow that was observed during the spring and early summer seasons.

The persistent patterns seen in the mid-depth currents that flow throughout the wedge-shaped region were not observed at site F (Figure 8). The subtidal currents are weak and disorganized at site F, which is northwest of site B but in the same water depth. The currents at site F are unusual in that they are weaker and have much higher frequency variability than currents observed elsewhere over the continental slope along the California coast. The currents at 150 m were smaller than the equivalent currents at site B, even though they do flow toward the northwest in the spring and early summer seasons. The poleward currents do not extend to 250 m. These characteristics suggest that site F was just east of the inshore boundary of the correlated, wedge-shaped flow field observed at the other sites on the slope.

The daily, mid-depth tidal currents have combined amplitudes less than 5 cm/s (Kinoshita, et al., 1992). The semidiurnal mid-depth tidal currents are a bit stronger, with combined amplitude that can reach 10 cm/s, but are generally less than 8 cm/s. Hence, neither of these tidal constituents can significantly alter the subtidal current regime described above. Their main effect is to increase the cross-slope current components. Hence material suspended in the water column will be dispersed across isobaths more easily than if the tidal current were absent.

#### *Deep currents over the slope*

Currents in water depths below 900 m occupy about half the water column at site E, the site chosen to characterize EPA's candidate dump area 5. This single measurement at 1420 m obtained of currents at depth suggests that deep currents over the slope are weak and variable. The subtidal deep currents are polarized alongslope, but their amplitudes tend to be less than 10 cm/s (Figure E). The mean current is 1 cm/s toward the northwest (Kinoshita et al., 1992). The amplitude is small, but the flow is persistent enough that the direction is significant for this year of record.

The tidal currents have amplitude that are somewhat smaller than those observed higher in the water column, amplitudes are less than 4 cm/s. But because the subtidal currents are also small, the tidal currents can act to reverse both the net along and cross-slope flow (Kinoshita, et al. 1992).

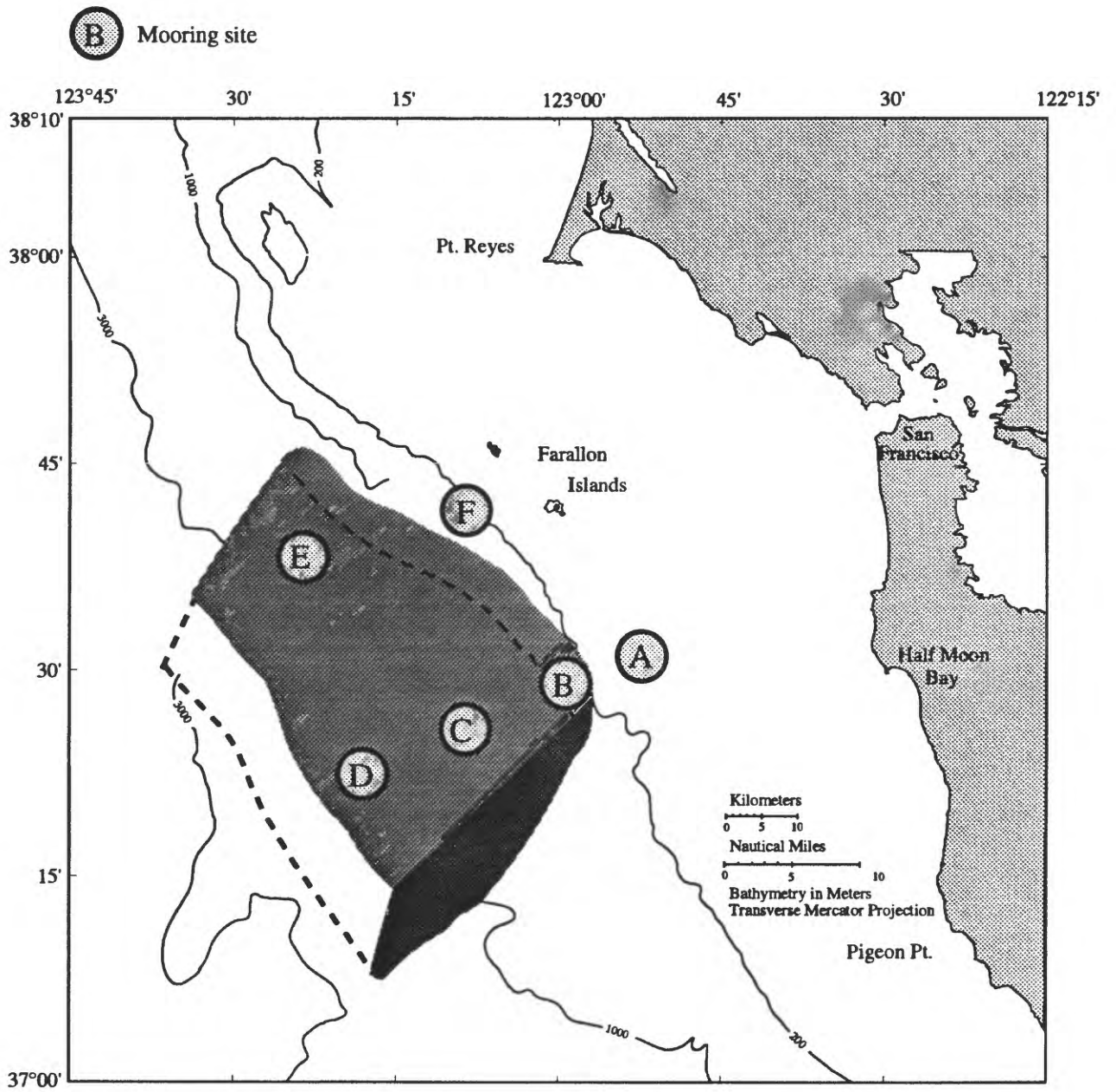


Figure 8. The "wedge" region of correlated mid-depth flow over the slope.

### *Near-bed currents over the slope*

The characteristics of subtidal currents within 20 m of the sea bed can not be reliably predicted from measurements made above them, for they are different from the currents in the overlying water column. The near-bed currents are also different from those measured at adjacent sites. For example, subtidal near-bed currents at site B appear unrelated to near-bed currents at site C, even though currents in the overlying water column share similar characteristics. (Figures B, C). These differences are not simply that the measurements were taken in different water depths. The differences arise because the near-bed currents are more strongly controlled by topographic features that currents higher in the water column.

The structure of the topography along the central line in the moored array, the line that contains sites A-D, shows that the bottom falls off toward the west, but the slope of the gradient is gentle compared to the slope found along the northern line (Figure 1). It is possible that this change in topography is one of the reasons that the core of the mid-depth flow discussed above veers offshore as the flow approaches the northern section of the moored array.

It is clear that the local structure of the topography strongly affects the near-bed currents. The subtidal near-bed currents flow along isobaths, but their amplitudes are much smaller than flow in the overlying water column at most sites on the slope (Figures B-E). The subtidal, near-bed currents at sites B and C range between 10 and 15 cm/s, while currents at 250 m reach speeds of 30 cm/s or more. The subtidal near-bed currents on the outer slope, at sites D and E and also small, but this can be expected in these deep water depths.

The subtidal near-bed currents at these 4 sites have very different temporal patterns. In contrast to the overlying flow, the subtidal near-bed currents at sites B and D have no definite seasonal or temporal patterns (Figures B, D). The mean currents are weakly equatorward, with speeds of 0.7 and 0.2 cm/s at B and D respectively. The mean flow is small enough that the direction is barely significant at B and not significant at D (Kinoshita, et al., 1992). In addition, the duration of a particular event in the near-bed currents last only a few days, a time period shorter than found in the overlying water column.

In contrast to these two sites, the near-bed subtidal flow at site C is persistently poleward for most of the observation period (Figure C). There are only a few, short periods when currents turn toward the southeast. The near-bed currents at site E also have a steady direction over time. They flow northeastward, across the general direction of the isobaths, toward the shelf (Figure E). This shoreward, near-bed flow at site E is caused by

interactions between the current and the local topography. Site E is located on the side of a small canyon. Currents at this site flow up the canyon.

One of the most interesting features of the observed tidal currents over the slope is the increase in amplitude of both diurnal and semidiurnal tidal constituents towards the bottom at some locations (Tables A7 and A8, Kinoshita et al., 1992). The semidiurnal species ( $M_2$  and  $S_2$ ) showed this response at sites B, C, E, and weakly at site D. The amplitudes at sites B, C, and E were 2-3 times the amplitudes at the instruments immediately above. The diurnal species ( $O_1$  and  $K_1$ ) showed this response at sites C and E only. This "bottom trapping" of the tidal currents was not unexpected since it was previously observed over the continental slope off Point Sur (Sielbeck, 1991). Amplification of semidiurnal tides may be due to the constructive interaction of free internal waves along preferred ray paths. This cannot explain the diurnal trapping however, since the diurnal frequency is subinertial off the Farallones and free internal waves cannot exist. These tides are likely trapped by a different, more complicated mechanism (Sielbeck, 1991; Rhines, 1970). The lack of amplification at mooring F may be explained by the unusually steep bottom slope there, which may not allow this trapping to occur.

The bottom trapping of diurnal and semidiurnal tides is important, since the tidal currents are 2-3 times greater at the bottom than they would be otherwise, and can resuspend larger grain-sized materials and transport them for greater distances than would occur in the absence of bottom trapping. The rectification of the bottom-enhanced tides by topographic features can also drive unusually strong mean flows which transport materials in a certain direction. This may be happening at 1987 m at site E, where a steady up-canyon mean flow was observed.

## DISCUSSION

The characteristics of the currents over the shelf and slope within and adjacent to the Gulf of the Farallones share similarities with currents observed in other regions of the California coast, but the exact current patterns are unique to this region. In particular, the near-surface flow over the slope is more poleward than was expected, tides can be larger and amplified at different frequencies than found in other areas, the California undercurrent can have a unique spatial pattern and there may be a non-local source for the upwelled waters found on the shelf. All these characteristics affect the resuspension, dispersal and ultimate fate of dredged materials deposited in this region. A discussion of the local circulation patterns and of their possible effect on deposited dredged materials is given below.

On the outer shelf, the tidal and subtidal currents combined to generate currents with speed greater than 45 cm/s near the bed. These currents are powerful enough to move fine sand. Hence, any dredged materials that have sizes of fine sand or smaller can be moved from the disposal area. In addition, large currents from surface waves are expected over the outer shelf during the year because the shelf is shallow enough that surface wave currents can reach the sea bed. It is well known that when currents from surface waves combine with lower frequency flows, the erosive potential of the currents is greatly enhanced (Grant and Madsen, 1979). If the erosive effect from surface waves that either propagate into the area as swell or are locally generated by storms is combined with the large currents observed near the bed, the erosive potential over the outer continental shelf is high. The tendency for flows near the bed to flow poleward, especially in winter when large surface waves are generated by winter storms, suggest that some fraction of any dredged material deposited in region 2 will eventually move along the isobaths into the Farallones Marine Sanctuary.

The specifics of the upwelling process will also affect dispersal of material suspended in the water column and the transport of that material onto the shelf. It was postulated at the beginning of this study that local upwelling would cause water from 100 to 200 m over the upper slope to be drawn onto the shelf in the spring and summer. The data set collected by the entire physical oceanographic team suggests that local upwelling in the Gulf of the Farallones is at best, relatively weaker than found at other sites along the California coast. Both the satellite and hydrographic data show that the majority of the cold, salty water on found on the shelf during summer is advected into the region from a strong upwelling center north of Point Reyes (Ramp et al., 1992; Hamilton, 1992). Hence, it is less likely here than other regions that materials suspended at depth over the upper slope will be locally upwelled onto the shelf.

The subtidal currents over the slope could be separated into 4 characteristic regimes separated by depth: near-surface, mid-depth, deep and near bottom. The near-surface currents were characterized by flow above 20 m. The mid-depth currents generally were found between 50 and 800 m. Deep currents were below mid-depth and the near-bed currents were within 20 m of the sea bed.

The subtidal, near-surface currents over the slope flowed poleward during most of the year. The strong poleward flow was not caused by wind forcing. During this period, the winds and near-surface currents move in opposite directions; winds are equatorward and currents are poleward. One portion of the poleward surface flow is likely to be the surface expression of the poleward flowing California

undercurrent discussed below. Other, as yet undetermined, process also drive the near-surface currents poleward, for strong poleward flow is observed in September, when the undercurrent is weak. A better description of these features must await further analysis.

The near-surface currents did not move uniformly poleward over the year. In March and April, 1991, equatorward currents, with speeds near the surface exceeding 40 cm/s, were observed. The flow event was seen to depths of 250 m, thought the magnitude of the event decreased with depth. During this period, the water in the upper 100 m over the inner and middle slope was colder and saltier than normal (Kinoshita et al., 1992; Ramp, et al., 1992). It is possible that a filament originated at Point Reyes and moved into the study region in April, for filaments have strong currents and are partially composed of colder, recently upwelled water from shelf areas to the north. The observed current patterns could also be caused by the inner edge of a medium sized, clockwise-rotating eddy embedded in the oceanic California Current System that impinged on the slope in April. Further analysis of the hydrographic and satellite data are needed to determine the correct hypothesis.

The mid-depth currents were characterized by strong, highly-correlated current over most of the study region. Only site F was outside this correlated flow region. The correlated mid-depth currents were usually found in a wedge-shaped region over the middle and outer slope. During the spring and summer, the flow over most of this region was persistently poleward. These poleward currents are undoubtedly an expression of the California undercurrent. Our data suggest that the undercurrent off of San Francisco flows northwestward in a broad band over the gently-sloping area near candidate dump site 3, in water depths down to 800 m. The undercurrent veers offshore to the north, possibly because the slope becomes much steeper at site F. The undercurrent does remain over the middle and outer slope, flowing past site E and through candidate dump site 5.

The data suggest that the California undercurrent has a seasonal cycle. It is strongest from March through mid-August. Although the undercurrent is usually confined to the mid-depth ranges, at times it encompasses the near-surface flow and drives the water at 10 m to the northwest. During other periods, the surface flow is uncoupled to that of the undercurrent. This uncoupling is especially noticeable at site B, on the inshore edge of the flow. The undercurrent either weakens or moves offshore of our measurement region in August through mid-November. There is no sign of a strong poleward flow during this time period. The data

suggest that the undercurrent begins to reform in December.

Because we have only one year of record, it is not known if the seasonal pattern we see for the undercurrent is typical for this region. There is only one short data record, taken at site E the previous year, that can provide more information (Noble, 1990). These short data records show that the subtidal flow does turn from poleward to equatorward in August, similar to the seasonal cycle inferred in this measurement program. Hence, previous measurements do support the observed pattern. However, even though the historical record supports the inferred seasonal cycle, they are too short to provide a definitive, confirming evidence.

The deep currents over the slope were the least energetic currents observed in this study. The combination of weak tidal and subtidal currents suggests that material suspended in the water column at depth would slowly disperse. The dispersal would take a much longer time than the equivalent dispersal at mid-depth.

The specific structures of the local topography caused enhanced flow and veering in the currents near the bed. The enhanced tidal currents were generally stronger than the subtidal near-bed currents. Hence, the enhanced tides provided the largest contribution to the erosive climate at the various sites. The near-bed currents have maximum speeds between 37 and 43 cm/s at sites B, C, and E, the sites with the largest near-bed tides. Maximum speeds are less at the other two sites. Hence, material deposited at sites B, C or E can be more preferentially eroded than material at sites D or F. The near-bed subtidal flow direction suggests that resuspended material at B will be dispersed in both directions along the isobaths. Resuspended material at C will be carried poleward and resuspended material at E will be carried up the canyon. Because site E is in 2000 m of water, it is not expected that resuspended material will move up the canyon to shallow shelf depths. Rather it will remain in the deeper portions of the canyon.

## CONCLUSIONS

The year-long measurement program of currents over the shelf and slope within and adjacent to the Gulf of the Farallones gathered a wealth of new information on the circulation patterns in this region. The current patterns suggest that flow over the shelf and slope are not strongly coupled. The strong, equatorward winds in the spring and summer drive shelf currents to the southeast, but are less effective in driving the near-surface currents over the slope. The upwelling process, which can move water in the upper layers from the slope to the shelf, is weaker here than at other areas on the California coast. The

current patterns also show that large currents, with speeds that often exceed 30 cm/s, can exist for extended periods of time above 800 m in the slope water. These currents weaken below 800 m, but can increase in amplitude again near the sea bed. The specific areas where strong, near-bed flows occur are controlled by local details in the topography. Small canyons or specific gradients in the slope of the local topography can both act to enhance currents near the bed.

The significant variations of the currents with depth and horizontal location indicate that the eventual fate of dredged materials deposited on the shelf or slope will be location dependent. Materials that reach the sea floor will disperse less in quiescent areas, typified by site D, than in energetic areas similar to site B. Materials that remain suspended for significant periods of time at depths less than 800 m over the slope will tend to travel long distances, for mid-depth slope currents are energetic. The direction of material transport will be seasonally dependent in a way that is not yet clear. For instance, the suspended material transport would have been mainly toward the northwest during May through August since the subtidal, mid-depth currents were mainly poleward. Later in the year, the current direction was more variable. Suspended material at depth will not move as far, because deep currents are weak.

The general patterns for the fate of dredged materials deposited at a specific location can be estimated from an analysis of the current records, but because the fate is critically dependent on circulation characteristics that change with horizontal and vertical location and time, some caution must be used in interpreting the results. The dredged material is also comprised of materials with many different characteristics, which further complicates the problem. A numerical model that incorporates both the current and particle size characteristics will give a more exact prediction of the fate of deposited dredged materials. One numerical model is currently being developed at SAIC. The output from this model will be available to the study group.

There is one strong caveat to the predictions of the fate of dredged material either from the current measurements alone or from a numerical model. Both rely strongly on the data gathered in this measurements program. While the data collected on currents over the slope is extensive, it only covers one year record. The process observed over the slope have time scales of six months or more. Because no other data is available, it is not yet known how typical the observed circulation patterns are. This consideration does not apply to models of dispersal over the shelf because the historical record of shelf currents is much more extensive. One can evaluate the candidate disposal sites relative to each other with this data, for major characteristics, such as the

presence or absence of enhanced near-bed flows are unlikely to change. However, more reliable predictive models of the fate of dredged materials can be developed if longer data sets are obtained of the currents over the slope.

## REFERENCES

- Brink, K. H., 1983. "The Near-Surface Dynamics of Coastal Upwelling." *Progress in Oceanography*, Vol. 12, p. 223 - 257.
- Brink, K. H., and T. Cowles, 1991: The Coastal Transition Zone Program. *J. of Geophys. Res.*, 96, 14,637-14,647.
- Brink, K. H., R. C. Beardsley, P. P. Niiler, M. R. Abbott, A. Huyer, S. R. Ramp, T. P. Stanton, and D. Stuart, 1991: Statistical properties of near surface flow in the California coastal transition zone. *J. Geophys. Res.*, 96, 14,693-14,706.
- Chelton, D. B., 1984. "Seasonal Variability of Alongshore Geostrophic Velocity of Central California." *J. of Geophys. Res.*, 89, p. 3473 - 3486.
- Chelton, D. B., A. W. Bratkovich, R. L. Bernstein, and P. M. Kosro, 1988. "Poleward Flow off Central California During the Spring and Summer of 1981 and 1984." *Journal of Geophysical Research*, Vol. 93, No. C9, pp. 10604 - 10620.
- Freeland, H. J., W. Jr., Crawford, and R. E. Thomson (1984): Currents along the Pacific Coast of Canada. *Atmos.-Oc.*, 22(2), 151-172.
- Freitag, H. P. and D. Halpern, 1977. "Hydrographic Observations off Northern California During May 1977." *Journal of Geophysical Research*, Vol. 86, p. 4248 - 4252.
- Grant, W. D. and O. S. Madsen, 1979. Combined wave and current interaction with a rough bottom. *Journal of Geophysical Research*, Vol. 84, p. 1797-1808.
- Hamilton, P. 1992. A compendium of satellite photographs in the Gulf of the Farallones, in prep.
- Hickey, B. M., 1979. "The California Current System - Hypotheses and Facts." *Progress in Oceanography*, Vol. 8, p. 191 - 279.
- Hickey, B. M., 1989: Poleward flow near the northern and southern boundaries of the U.S. West Coast. In: *Poleward flows along eastern ocean boundaries*. Springer-Verlag Coastal and Estuarine Studies Vol. 34. S. J. Neshyba, C. N. K. Mooers, R. L. Smith, and R. T. Barber, editors. 374 p.
- Huyer, A., R. L. Smith, and E. J. C. Sobey, 1978: Seasonal differences in low-frequency current fluctuations over the Oregon continental shelf. *J. Geophys. Res.*, 83, 5077-5089.
- Huyer, A., 1983. "Coastal Upwelling in the California Current System." *Progress in Oceanography*, Vol. 12, p. 259 - 284.
- Huyer, A., R. L. Smith, and B. M. Hickey, 1984: Observations of a warm-core eddy off Oregon, January-March 1978. *Deep Sea Res.*, 31, 97-117.
- Huyer, A., and R. L. Smith, 1985: The signature of El Nino off Oregon, 1982-83. *J. Geophys. Res.*, 90, 7133-7142.
- Huyer, A., P. M. Kosro, S. Lentz, and R. C. Beardsley, 1989: Poleward flows in the California Current System. In: *Poleward flows along eastern ocean boundaries*. Springer-Verlag Coastal and Estuarine Studies Vol. 34. S. J. Neshyba, C. N. K. Mooers, R. L. Smith, and R. T. Barber, editors. 374 p.
- Huyer, A., P. M. Kosro, J. Fleischbein, S. R. Ramp, T. Stanton, L. Washburn, F. P. Chavez, T. J. Cowles, S. D. Pierce, and R. L. Smith, 1991: Currents and water masses of the coastal transition zone off northern California, June to August 1988. *J. Geophys. Res.*, 96, 14,809-14,832.
- Kinoshita, K. L., M. A. Noble and S. R. Ramp, 1992: The Farallones moored array data report. in preparation.
- Kosro, P. M., 1987. "Structure of the Coastal Current Field off Northern California During the Coastal Ocean Dynamics Experiment." *Journal of Geophysical Research*, Vol. 92, No. C2, p. 1637 - 1654.
- Lentz, S. J., editor, 1991. The coastal ocean dynamics experiment (CODE). Collected Reprints.
- Lynn, R. J., and J. J. Simpson, 1990. "The flow of the undercurrent over the continental borderland off Southern California." *Journal of Geophysical Research*, Vol. 95, No. C8, 12,955-13,008.
- McCreary, J. P. Jr., P. Kundu, and S.-Y. Chao, 1987. "The Dynamics of the California Current System." *Journal of Marine Research*, Vol. 45, pp. 1-32.
- Mooers, C. N. K., and A. R. Robinson, 1984. "Turbulent Jets and Eddies in the California Current and Inferred Cross-Shore Transports." *Science*, Vol. 223, p. 51 - 53.
- Neshyba, S. J., C. N. K. Mooers, R. L. Smith, and R. T. Barber, editors. 1989: *Poleward flows along eastern ocean boundaries*. Springer-Verlag Coastal and Estuarine Studies Vol. 34., 374 p
- Noble, M. and G. Gelfenbaum, 1990: A pilot study of currents and suspended sediment in the Gulf of the Farallones. U. S. Geological Survey Open File Report 90-476.
- Noble, M., 1990. Currents over the slope off San Francisco CA. Report by the U.S. Geological Survey for the U. S. Navy.
- Pares-Sierra, A., and J. J. O'Brien, 1989. "The Seasonal and Interannual Variability of the California Current system: A Numerical Model." *Journal of Geophysical Research*, Vol. 94, No. C3, pp. 3159 - 3180.

- Ramp, S. R., P. F. Jessen, K. H. Brink, P. P. Niiler, F. L. Daggett, and J. S. Best, 1991: The physical structure of cold filaments near Point Arena, California, during June 1987. *J. Geophys. Res.*, 96, 14,859-14,884.
- Ramp, S. R., N. Garfield, C. A. Collins, L. K. Rosenfeld, and F. B. Schwing, 1992: Circulation studies over the continental shelf and slope near the Farallon Islands, CA. Executive summary, EPA report, in prep.
- Rienecker, M. M., C. N. K. Mooers, and A. R. Robinson, 1987. "Dynamical Interpolation and Forecast of the Evolution of Mesoscale Features off Northern California." *Journal of Physical Oceanography*, Vol. 17, No. 8, pp. 1189 - 1213.
- Rienecker, M. M., and C. N. K. Mooers, 1989. "Mesoscale eddies, jets, and fronts off Point Arena, CA, July 1986. *Journal of Geophysical Research*, Vol. 94, 12,555-12,570.
- Rhine, P., 1970: Edge, bottom, and Rossby waves in a rotating stratified fluid. *J. Geophys. Fluid Dynamics*, 1, 273-302.
- Send, U., R. C. Beardsley, and C. D. Winant, 1987. "Relaxation From Upwelling in the Coastal Ocean Dynamics Experiment." *Journal of Geophysical Research*, Vol. 92, No. C2, p. 1683 - 1698.
- Sherwood, C. R., D. A. Coats, D. W. Denbo and J. P. Downing, 1990. Physical oceanographic processes at candidate dredged-material di Kinoshita, et al, 1992 San Francisco. Battelle Northwest Laboratory, Sequim Washington.
- Sielbeck, S. L. 1991: Bottom trapped waves at tidal frequencies off Point Sur, Ca. Naval Postgraduate School, Monterey, CA., 62 p.
- Strub, P. T., J. S. Allen, A. Huyer, R. L. Smith, and R. C. Beardsley, 1987. Seasonal cycles of currents, temperature, winds and sea level over the northern Pacific continental shelf: 35°N to 48°N. *Journal of Geophysical Research*, Vol. 92, No. C2, p. 1507 - 1526.
- Tisch, T. D., S. R. Ramp, and C. A. Collins: Observations of the geostrophic current and water mass characteristics off Point Sur, California from May 1988 through November 1989. Submitted to *J. Geophys. Res.*
- Winant, C. D., R. C. Beardsley, and R. E. Davis, 1987. "Moored Wind, Temperature, and Current Observations Made During Coastal Ocean Dynamics Experiments 1 and 2 Over the Northern California Continental Shelf and Upper Slope." *Journal of Geophysical Research*, Vol. 92, No. C2, p. 1569 - 1604.
- Wyrtki, K., 1965: Summary of the physical oceanography of the Eastern Pacific Ocean. Institute of Marine Resources, University of California, San Diego, Ref. 65-10, 78 pp.

## **APPENDIX**

- Figure A. Subtidal currents at site A.**
- Figure B. Subtidal currents at site B.**
- Figure C. Subtidal currents at site C.**
- Figure D. Subtidal currents at site D.**
- Figure E. Subtidal currents at site E.**
- Figure F. Subtidal currents at site F.**

Site A

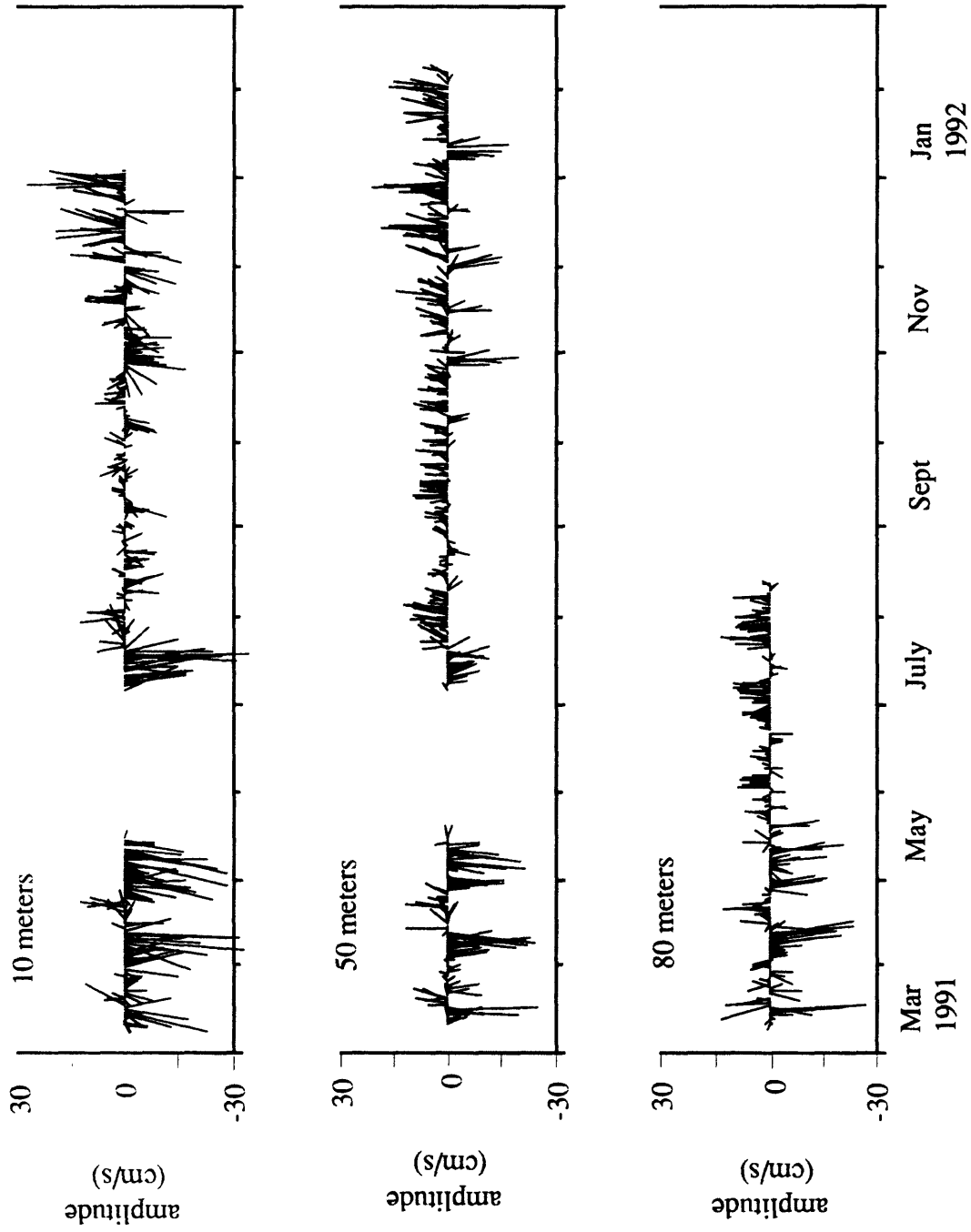


Figure A. Subtidal currents at site A. Each line represents the magnitude and orientation of the current vector. A line pointing toward the top of the page represents poleward flow along the shelf. Currents flowing toward the coast point to the right.

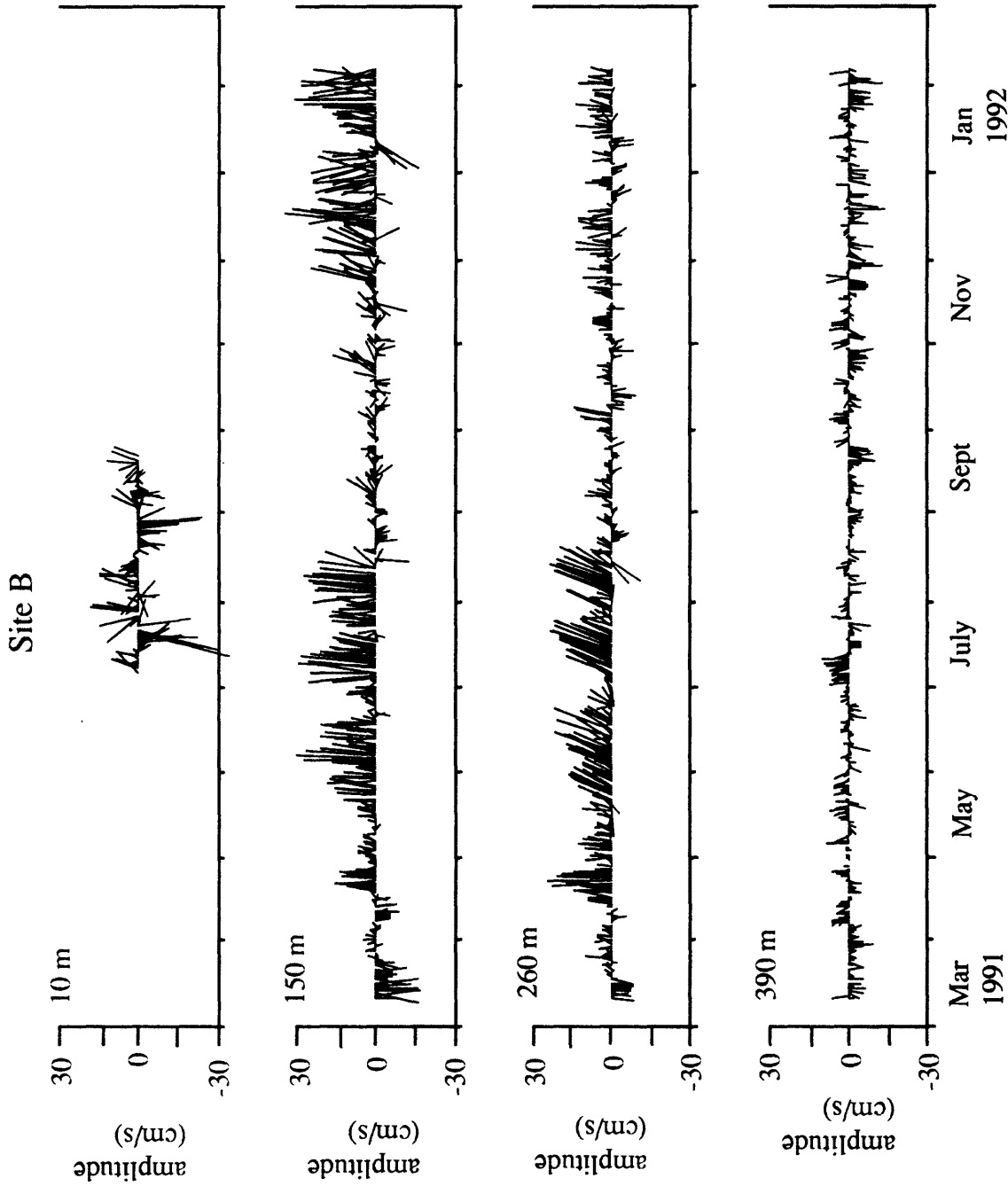


Figure B. Subtidal currents at site B. Each line represents the magnitude and orientation of the current vector. A line pointing toward the top of the page represents poleward flow along the slope. Currents flowing toward the coast point to the right.

Site C

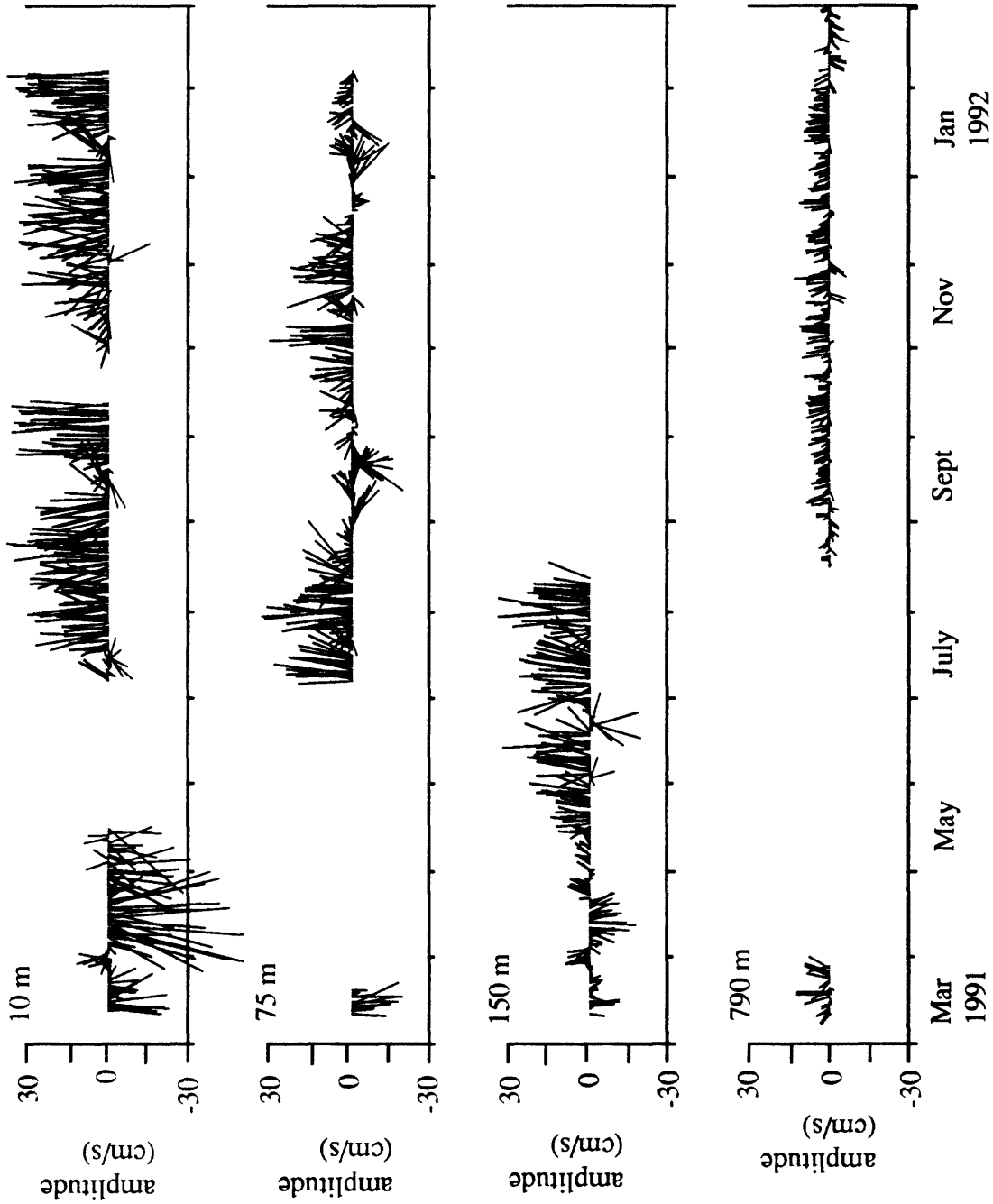


Figure C. Subtidal currents at site C. Each line represents the magnitude and orientation of the current vector. A line pointing toward the top of the page represents poleward flow along the slope. Currents flowing toward the coast point to the right.

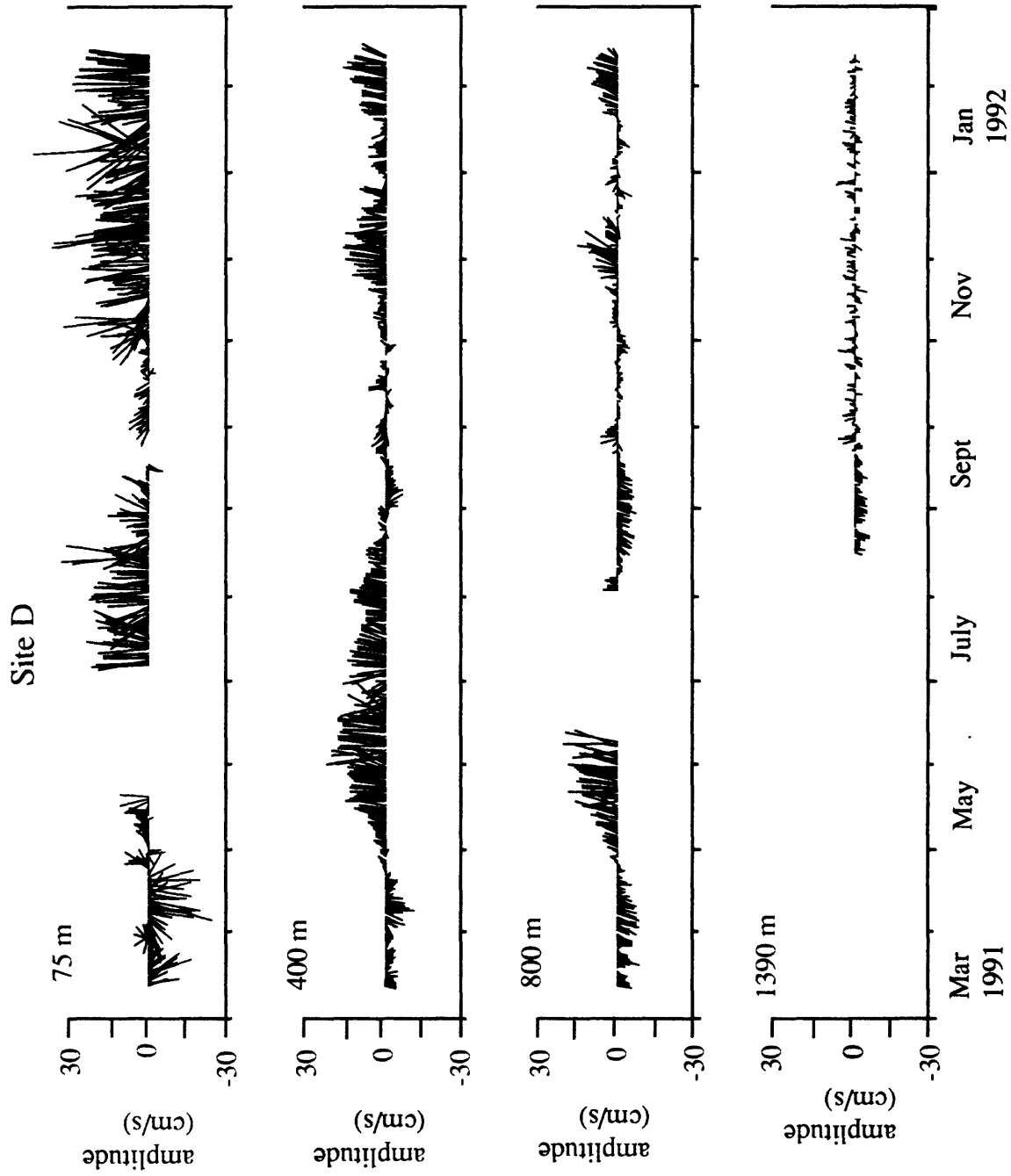


Figure D. Subtidal currents at site D. Each line represents the magnitude and orientation of the current vector. A line pointing toward the top of the page represents poleward flow along the slope. Currents flowing toward the coast point to the right.

Site E

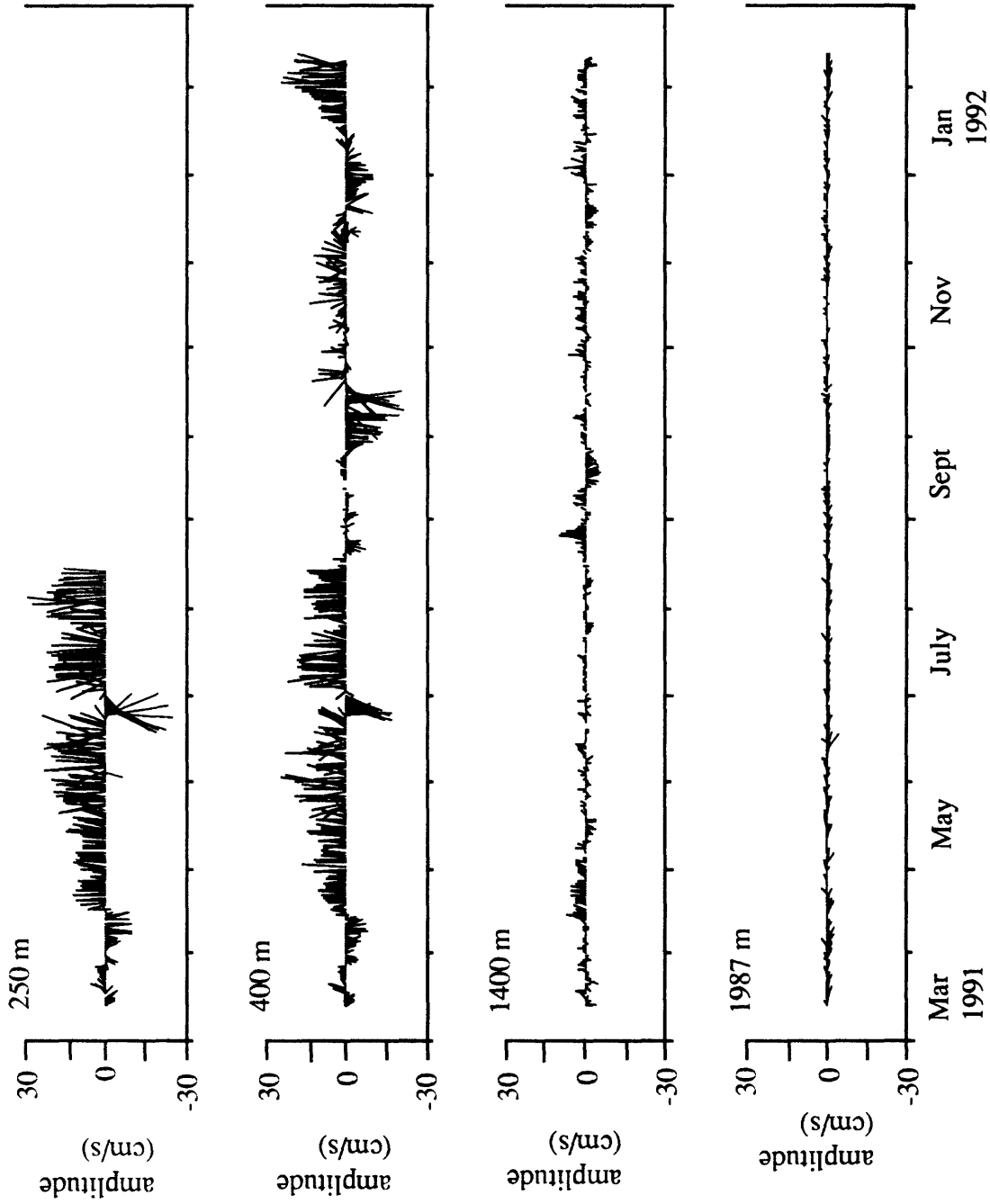


Figure E. Subtidal currents at site E. Each line represents the magnitude and orientation of the current vector. A line pointing toward the top of the page represents poleward flow along the slope. Currents flowing toward the coast point to the right.

Site F

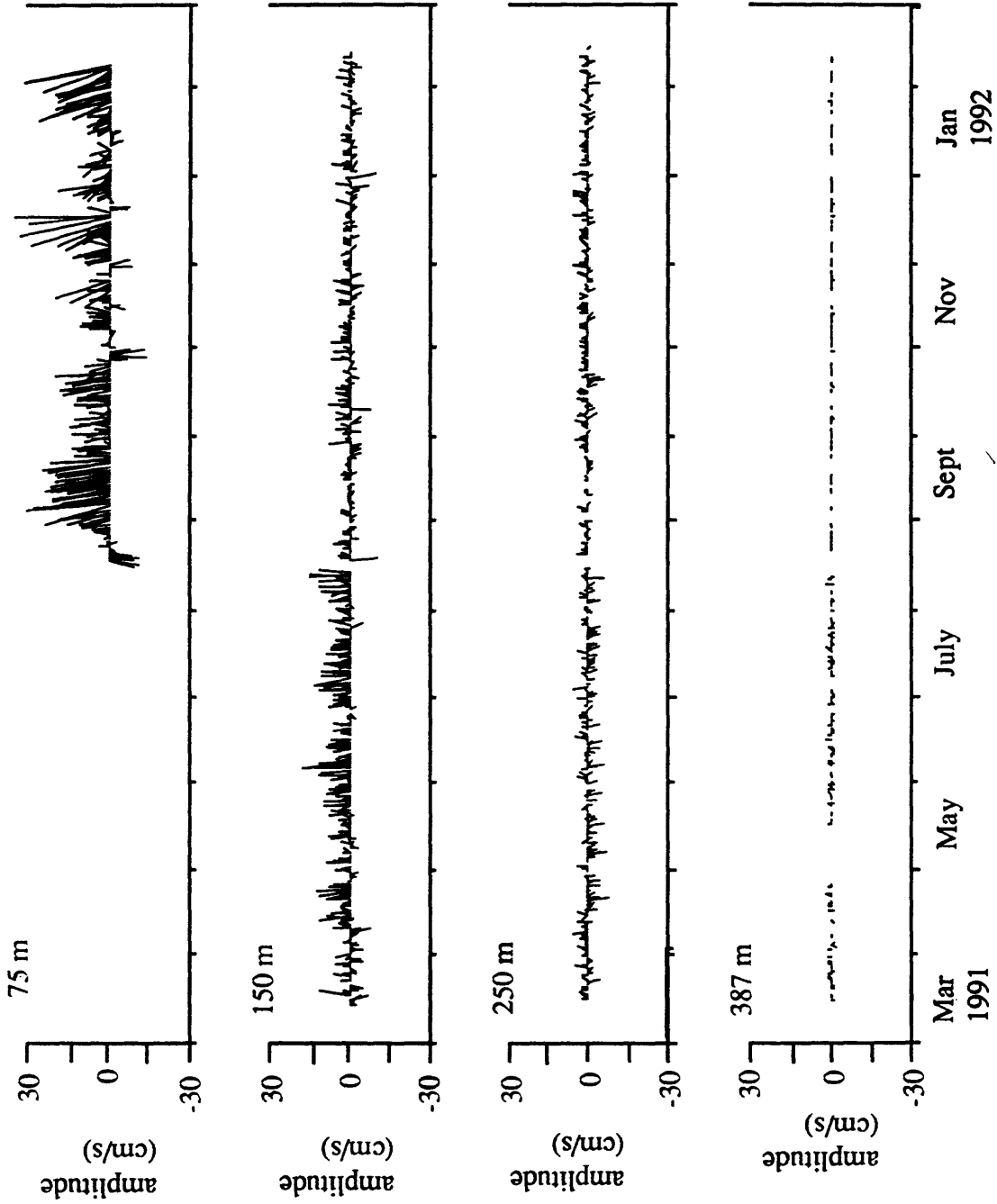


Figure F. Subtidal currents at site F. Each line represents the magnitude and orientation of the current vector. A line pointing toward the top of the page represents poleward flow along the slope. Currents flowing toward the coast point to the right.